International Journal of Power Electronics and Drive System (IJPEDS)
Vol. 10, No. 2, June 2019, pp. 1022~1033
ISSN: 2088-8694, DOI: 10.11591/ijpeds.v10.i2.pp1022-1033

Current control of grid-connected inverter using integral sliding mode control and resonant compensation

Seung-Jin Yoon, Thanh Van Nguyen, Kyeong-Hwa Kim
Department of Electrical and Information Engineering, Seoul National University of Science and Technology, Korea

Article Info

Article history:

Received Nov 17, 2018
Revised Jan 22, 2019
Accepted Mar 7, 2019

Keywords:

Distributed generation
Grid-connected inverter
Indirect current control
Integral sliding mode control
Power quality

ABSTRACT

To eliminate the adverse effect from parameter variations as well as distorted grid conditions, a current control scheme of an LCL-filtered grid-connected inverter using a discrete Integral Sliding Mode Control (ISMC) and resonant compensation is presented. The proposed scheme is constructed based on the cascaded multiloop structure, in which three control loops are composed of grid-side current control, capacitor voltage control, and inverter-side current control. An active damping to suppress the resonance caused by LCL filter can be effectively realized by means of the inverter-side feedback control loop. Furthermore, the seamless transfer operation between the grid-connected mode and islanded mode is achieved by the capacitor voltage control loop. To retain a high tracking performance and robustness of the ISMC as well as an excellent harmonic compensation capability of the Resonant Control (RC) scheme at the same time, two control methods are combined in the proposed current controller. As a result, the proposed scheme yields a high quality of the injected grid currents and fast dynamic response even under distorted grid conditions. Furthermore, to reduce the number of sensors, a discrete-time reduced-order state observer is introduced. Simulation and experimental results are presented to demonstrate the effectiveness of the proposed scheme.

Copyright © 2019 Institute of Advanced Engineering and Science.
All rights reserved.

Corresponding Author:

Kyeong-Hwa Kim,
Department of Electrical and Information Engineering,
Seoul National University of Science and Technology,
232 Gongneung-ro, Nowon-gu, Seoul, 01811, Korea.
Email: k2h1@seoultech.ac.kr

1. INTRODUCTION

In recent years, renewable energy sources (RESs) such as wind and solar are attracting great attentions due to the depletion of fossil energy and environmental issues [1-3]. To integrate various RESs into the utility grid, Distributed Generation (DG) systems as a component of microgrid (MG) has been developed [4]. With the advantages of easy integration of resources, flexible installation location, and reliable operation, DG-based MG becomes a future trend of constructing the electric power system [5]. Basically, MG is formed by connecting DG units with energy storage system and local loads. To interface DG units with the utility grid, the Interlinking Converters (ICs) are usually employed. Currently, most of ICs adopt a Voltage Source Inverter (VSI) with current control to regulate the current injected into the grid. The grid-connected VSI should be controlled to achieve a high performance of injected grid currents in the sense of fast dynamic response, robustness to perturbation, zero tracking error, and low Total Harmonic Distortion (THD).

With the aim of attenuating the harmonic components caused by the pulse width modulation (PWM), the filter is connected between the utility grid and VSI [6]. In recent years, LCL filters are widely applied to a grid-connected inverter system because they provide a better harmonic attenuation capability [7]. Moreover, LCL filter has lower cost and smaller physical size in comparison to L filter to achieve the same

harmonic attenuation. Due to this advantage, the study of LCL filter has been a topic of intense research mainly in terms of design and development of control methods. However, because the LCL filter causes the resonance problem, a current control strategy of an LCL-filtered grid-connected inverter should be carefully designed to stabilize the system.

The resonance problem of LCL filter can be dealt with by two main methods, namely, the passive damping and active damping. The passive damping is simply achieved by adding a resistor in series with the filter capacitor [8]. Despite simple implementation, this method causes extra losses through heat dissipation, resulting in reduced system efficiency. To overcome such a limitation, the active damping technique which damps the resonance by a control algorithm has been introduced. To stabilize an inverter system without increasing the loss, an active damping approach based on a virtual resistance has been studied by using the filter capacitance current feedback [9]. However, this scheme requires extra sensors to measure the capacitor currents, which leads to the cost increase and hardware complexity of system.

To provide uninterruptable power to the critical load even in the occurrence of utility outage, the grid-connected inverter should operate in both the grid-connected mode and islanded mode [10]. In the grid-connected mode, the inverter is operated with current-controlled mode to inject the power into the utility grid, while the critical load voltage is maintained by the grid voltage. Once the utility fault occurs, the inverter operation is switched into the islanded mode, in which the inverter is operated with the voltage-controlled mode. The transition between these two control modes should be seamless to prevent the load damage due to unstable load voltage. For this purpose, a multiloop indirect current control method has been presented as one of the effective approaches. The seamless transfer is achieved by combining the outer control loop of grid-side current and inner control loop of filter capacitor voltage in [11]. By controlling the capacitor voltage in both the grid-connected and islanded modes, this method is capable of supplying the critical load with a stable and seamless voltage during the whole period. However, the control design is quite complicated. Furthermore, this scheme requires extra sensing devices to implement additional control loops. In addition, the adverse grid voltages such as the harmonic distortion have not been addressed.

To control the grid-connected inverter, the proportional-integral (PI) decoupling control has been widely used with the voltage feedforward because of its simplicity and stability. However, since the conventional PI decoupling control inherently has a poor disturbance rejection capability, it is not a suitable way to control grid-connected inverters under grid voltage perturbed by disturbances. To improve the power quality of inverter system, several studies have been investigated regarding the harmonic compensation strategy. The harmonic compensation can be achieved by two methods, namely, selective and non-selective schemes. As a selective harmonic compensation scheme, the proportional-resonant (PR) controller is widely employed because it provides a good reference tracking as well as harmonic compensation [12]. However, as the compensated harmonic terms are increased, the computational burden is also increased due to the implementation of separate resonant controllers.

As a non-selective harmonic compensation strategy, the predictive control [13] and repetitive control [14] schemes have been studied. Although the predictive control has a capability of providing fast dynamic response with minimum THD level, it is very sensitive to system parameter change. The repetitive control provides a good harmonic rejection for nonlinear loads with periodic distortions. However, slow dynamic response is the main shortcoming of this type of controller due to the learning process. To overcome the drawbacks of the aforementioned approaches, a nonlinear control strategy such as a sliding mode control (SMC) has been presented. Since the SMC is inherently insensitive to the presence of parameter uncertainties and external disturbances, many studies have been carried out to apply the SMC technique to grid-connected inverters [15-17]. A SMC scheme based on dual-loop control structure is presented in [15]. This approach not only guarantees the system stability, but also alleviates the chattering phenomenon effectively. In order to enhance the tracking performance and reduce the THD of injected grid currents effectively, a SMC scheme combined with multiple resonant terms is proposed in [16]. However, the implementation of this scheme is complicated in practice since it employs many resonant terms in the sliding surface function. Moreover, this approach requires several sensing devices to measure the inverter-side currents and capacitor voltages, which increases the system cost and hardware complexity. To eliminate the steady-state error, an integral sliding mode control (ISMC) is designed by using the continuous-time model [17], in which the integral term is added into the sliding function. For easiness in implementation by digital controller, a discrete SMC approach is developed for grid-connected inverters [18], [19].

This paper presents a current control scheme for a three-phase LCL-filtered grid-connected inverter based on a discrete integral sliding mode control (ISMC) combined with resonant compensation. The proposed control scheme is constructed by using the multiloop indirect control structure which is composed of the grid-side current control loop, capacitor voltage control loop, and inverter-side current control loop. By adding the capacitor voltage control loop into the control structure, the seamless transfer between the grid-connected mode and islanded mode can be achieved. In addition, a discrete-time reduced-order state observer

is introduced with the aim of reducing the total number of sensing devices. In the proposed control scheme, the active damping is realized through a feedback control loop of inverter-side current by using the estimated inverter-side current from the state observer. As a result, the proposed control scheme not only ensures the stability by active damping but also reduces the system cost since the use of additional sensing devices can be avoided. With the motivation to improve the current quality injected into the grid under harmonically distorted grid voltage, the resonant controllers (RCs) are combined with the discrete ISMC in outer-loop grid-side current controller in the discrete-time domain. While the robustness and fast dynamic response of grid current control are ensured by the discrete ISMC, a high quality of current with low THD is achieved by the harmonic compensation based on the RC. To verify the effectiveness and validity of the proposed current control scheme, the PSIM software-based simulations and experiments have been carried out by using three-phase 2 kVA prototype grid-connected inverter. The entire control algorithm is implemented on a digital signal processor (DSP) TMS320F28335 and tested under distorted grid conditions. This paper is organized as follows. Section 2 presents the modeling of inverter. Section 3 explains the proposed discrete ISMC scheme with the harmonic compensation. In section 4, the simulations and experimental results are presented. Finally, this paper is concluded in Section 5.

2. MODELING OF LCL-FILTERED GRID-CONNECTED INVERTER

Figure 1 shows a configuration of a three-phase grid-connected inverter connected to the grid through an LCL filter, in which V_{DC} represents the DC link voltage, R_1 and R_2 are the filter resistances, L_1 and L_2 are the filter inductances, and C_f is the filter capacitance. The state equations of the grid-connected inverter are expressed in the synchronous reference frame (SRF) as follows:

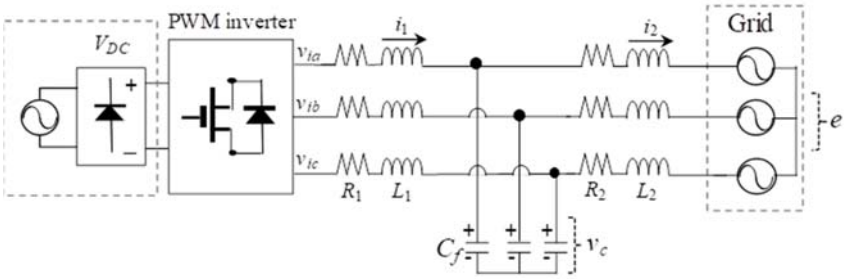

Figure 1. Configuration of three-phase grid-connected inverter with LCL filter

$$\frac{d}{dt}\begin{bmatrix} i_{2q} \\ i_{2d} \end{bmatrix} = \begin{bmatrix} -R_2/L_2 & -\omega \\ \omega & -R_2/L_2 \end{bmatrix} \cdot \begin{bmatrix} i_{2q} \\ i_{2d} \end{bmatrix} + \begin{bmatrix} 1/L_2 & 0 \\ 0 & 1/L_2 \end{bmatrix} \cdot \begin{bmatrix} v_{cq} \\ v_{cd} \end{bmatrix} + \begin{bmatrix} -1/L_2 & 0 \\ 0 & -1/L_2 \end{bmatrix} \cdot \begin{bmatrix} e_q \\ e_d \end{bmatrix} \quad (1)$$

$$\frac{d}{dt}\begin{bmatrix} i_{1q} \\ i_{1d} \end{bmatrix} = \begin{bmatrix} R_1/L_1 & -\omega \\ \omega & R_1/L_1 \end{bmatrix} \cdot \begin{bmatrix} i_{1q} \\ i_{1d} \end{bmatrix} + \begin{bmatrix} -1/L_1 & 0 \\ 0 & -1/L_1 \end{bmatrix} \cdot \begin{bmatrix} v_{cq} \\ v_{cd} \end{bmatrix} + \begin{bmatrix} -1/L_1 & 0 \\ 0 & -1/L_1 \end{bmatrix} \cdot \begin{bmatrix} v_{iq} \\ v_{id} \end{bmatrix} \quad (2)$$

$$\frac{d}{dt}\begin{bmatrix} v_{cq} \\ v_{cd} \end{bmatrix} = \begin{bmatrix} 0 & -\omega \\ \omega & 0 \end{bmatrix} \cdot \begin{bmatrix} v_{cq} \\ v_{cd} \end{bmatrix} + \begin{bmatrix} -1/C_f & 0 \\ 0 & -1/C_f \end{bmatrix} \cdot \begin{bmatrix} i_{2q} \\ i_{2d} \end{bmatrix} + \begin{bmatrix} 1/C_f & 0 \\ 0 & 1/C_f \end{bmatrix} \cdot \begin{bmatrix} i_{1q} \\ i_{1d} \end{bmatrix} \quad (3)$$

where the subscripts "q" and "d" denote the variables in the SRF, $[i_{2q}\ i_{2d}]^T$ is the grid-side current vector, $[i_{1q}\ i_{1d}]^T$ is the inverter-side current vector, $[v_{cq}\ v_{cd}]^T$ is the capacitor voltage vector, $[e_q\ e_d]^T$ is the grid voltage vector, $[v_{iq}\ v_{id}]^T$ is the inverter output voltage, and ω is the angular frequency of the grid voltage. From (1) to (3), the continuous-time model of inverter system can be expressed in the SRF as;

$$\dot{\boldsymbol{x}}(t) = \boldsymbol{A}\boldsymbol{x}(t) + \boldsymbol{B}\boldsymbol{u}(t) + \boldsymbol{D}\boldsymbol{e}(t) \quad (4)$$

$$\boldsymbol{y}(t) = \boldsymbol{C}\boldsymbol{x}(t) \tag{5}$$

where $\boldsymbol{x} = [i_{2q}\ i_{2d}\ i_{1q}\ i_{1d}\ v_{cq}\ v_{cd}]^T$, $\boldsymbol{u} = [v_{iq}\ v_{id}]^T$, $\boldsymbol{e} = [e_q\ e_d]^T$, and the system matrices $\boldsymbol{A}$, $\boldsymbol{B}$, $\boldsymbol{C}$ and $\boldsymbol{D}$ are expressed as

$$\boldsymbol{A} = \begin{bmatrix} -R_2/L_2 & -\omega & 0 & 0 & 1/L_2 & 0 \\ \omega & -R_2/L_2 & 0 & 0 & 0 & 1/L_2 \\ 0 & 0 & -R_1/L_1 & -\omega & -1/L_1 & 0 \\ 0 & 0 & \omega & -R_1/L_1 & 0 & -1/L_1 \\ -1/C_f & 0 & 1/C_f & 0 & 0 & -\omega \\ 0 & -1/C_f & 0 & 1/C_f & \omega & 0 \end{bmatrix}$$

$$\boldsymbol{B} = \begin{bmatrix} 0 & 0 \\ 0 & 0 \\ 1/L_1 & 0 \\ 0 & 1/L_1 \\ 0 & 0 \\ 0 & 0 \end{bmatrix},\ \boldsymbol{D} = \begin{bmatrix} -1/L_2 & 0 \\ 0 & -1/L_2 \\ 0 & 0 \\ 0 & 0 \\ 0 & 0 \\ 0 & 0 \end{bmatrix},\ \boldsymbol{C} = \begin{bmatrix} 1 & 0 & 0 & 0 & 0 & 0 \\ 0 & 1 & 0 & 0 & 0 & 0 \end{bmatrix}.$$

For a digital implementation, the continuous-time model of the inverter system can be discretized as

$$\boldsymbol{x}(k+1) = \boldsymbol{A}_d\boldsymbol{x}(k) + \boldsymbol{B}_d\boldsymbol{u}(k) + \boldsymbol{D}_d\boldsymbol{e}(k) \tag{6}$$

$$\boldsymbol{y}(k) = \boldsymbol{C}_d\boldsymbol{x}(k) \tag{7}$$

where the matrices $\boldsymbol{A}_d$, $\boldsymbol{B}_d$, $\boldsymbol{C}_d$, and $\boldsymbol{D}_d$ can be calculated with the sampling period T_s as

$$\boldsymbol{A}_d = e^{\boldsymbol{A}T_s} = \boldsymbol{I} + \frac{\boldsymbol{A}T_s}{1!} + \frac{\boldsymbol{A}^2T_s^2}{2!} + \cdots \tag{8}$$

$$\boldsymbol{B}_d = \boldsymbol{A}^{-1}(\boldsymbol{A}_d - \boldsymbol{I})\boldsymbol{B},\ \boldsymbol{C}_d = \boldsymbol{C} \tag{9}$$

$$\boldsymbol{D}_d = \boldsymbol{A}^{-1}(\boldsymbol{A}_d - \boldsymbol{I})\boldsymbol{D}. \tag{10}$$

3. PROPOSED DISCRETE SLIDING MODE CONTROL WITH HARMONIC COMPENSATION

Figure 2 shows the overall block diagram of the proposed control scheme for an LCL-filtered three-phase grid-connected inverter. The proposed control scheme mainly consists of an ISMC, resonant compensation, and reduced-order observer in the discrete-time domain. The inverter reference voltages by the proposed current controller are applied through the space vector PWM. The proposed control scheme requires the measurement of only the grid-side currents and grid voltages. The measured grid voltages are used in the phase-locked loop (PLL) scheme to determine the grid phase angle.

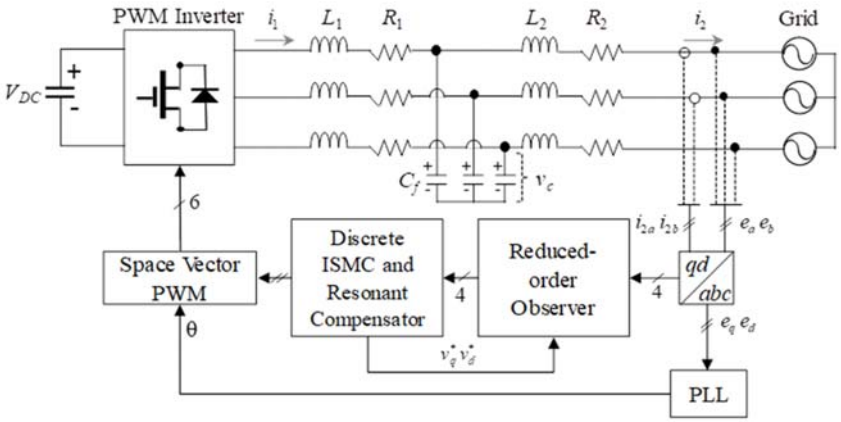

Figure 2. LCL-filtered three-phase grid-connected inverter and the proposed control scheme

Figure 3 shows the proposed current control scheme for the *q*-axis current based on the multiloop structure. To realize a cascaded multiloop controller, all the system states should be available for feedback purpose. However, additional sensing devices usually increase the total cost and hardware complexity in a practical inverter system. Therefore, a discrete-time reduced-order state observer is employed to obtain the estimated signals for the inverter-side currents and the capacitor voltages in the proposed control scheme. The discrete-time inverter model in (6) and (7) can be rewritten as

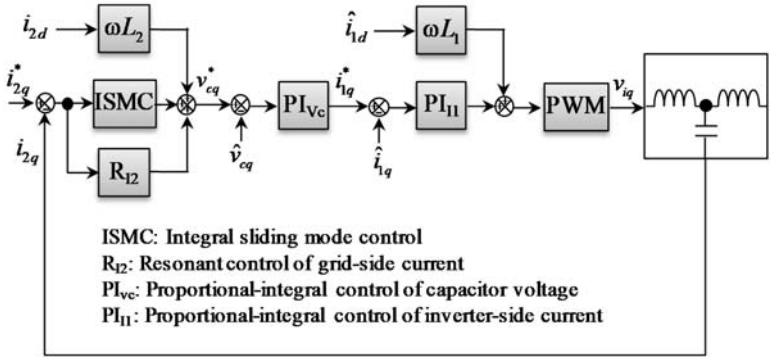

Figure 3. Proposed current control scheme; *q*-axis current control

$$\begin{bmatrix} \boldsymbol{x}_1(k+1) \\ \boldsymbol{x}_2(k+1) \end{bmatrix} = \begin{bmatrix} \boldsymbol{A}_{11} & \boldsymbol{A}_{12} \\ \boldsymbol{A}_{21} & \boldsymbol{A}_{22} \end{bmatrix} \begin{bmatrix} \boldsymbol{x}_1(k) \\ \boldsymbol{x}_2(k) \end{bmatrix} + \begin{bmatrix} \boldsymbol{B}_1(k) \\ \boldsymbol{B}_2(k) \end{bmatrix} \boldsymbol{u}(k) + \begin{bmatrix} \boldsymbol{D}_1(k) \\ \boldsymbol{D}_2(k) \end{bmatrix} \boldsymbol{e}(k) \tag{11}$$

$$\boldsymbol{y}(k) = \begin{bmatrix} \boldsymbol{C}_1 & \boldsymbol{C}_2 \end{bmatrix} \begin{bmatrix} \boldsymbol{x}_1(k) \\ \boldsymbol{x}_2(k) \end{bmatrix} \tag{12}$$

where $\boldsymbol{x}_1 = [i_{2q}\ i_{2d}]^T$ and $\boldsymbol{x}_2 = [i_{1q}\ i_{1d}\ v_{cq}\ v_{cd}]^T$. Then, the estimated state variables can be obtained by applying the discrete-time reduced-order state observer as [20]

$$\hat{\boldsymbol{x}}_2(k) = \boldsymbol{\eta}(k) + \boldsymbol{K}\boldsymbol{x}_1(k) \tag{13}$$

$$\begin{aligned} \boldsymbol{\eta}(k+1) = {} & (\boldsymbol{A}_{22} - \boldsymbol{K}\boldsymbol{A}_{12})\boldsymbol{\eta}(k) + (\boldsymbol{A}_{22} - \boldsymbol{K}\boldsymbol{A}_{12})\boldsymbol{K}\boldsymbol{y}(k) + (\boldsymbol{A}_{21} - \boldsymbol{K}\boldsymbol{A}_{11})\boldsymbol{y}(k) \\ & + (\boldsymbol{B}_2 - \boldsymbol{K}\boldsymbol{B}_1)\boldsymbol{u}(k) + (\boldsymbol{D}_2 - \boldsymbol{K}\boldsymbol{D}_1)\boldsymbol{e}(k) \end{aligned} \tag{14}$$

where the symbol "^" denotes the estimated variables and $\boldsymbol{K}$ is the observer gain matrix. The estimated variables $\hat{\boldsymbol{x}}_2$ are used in the multiloop control structure in Figure 3 instead of actual measurements.

To control the grid-side currents with a good disturbance rejection, an ISMC and resonant compensation are designed in the discrete-time domain. From (1), the state model of a grid-side current is expressed in the SRF as follows:

$$\dot{\boldsymbol{x}}_1(t) = \boldsymbol{A}_g \boldsymbol{x}_1 + \boldsymbol{B}_g \boldsymbol{v}_c + \boldsymbol{D}_g \boldsymbol{e} \tag{15}$$

where $\boldsymbol{v}_c = [v_{cq}\ v_{cd}]^T$

$$\boldsymbol{A}_g = \begin{bmatrix} -R/L_2 & -\omega \\ \omega & -R/L_2 \end{bmatrix},\ \boldsymbol{B}_g = \begin{bmatrix} 1/L_2 & 0 \\ 0 & 1/L_2 \end{bmatrix},\ \boldsymbol{D}_g = \begin{bmatrix} -1/L_2 & 0 \\ 0 & -1/L_2 \end{bmatrix}. \tag{16}$$

The continuous-time model of grid-side current can be similarly discretized by using (8) - (10) as

$$\boldsymbol{x}_1(k+1) = \boldsymbol{A}_{dg} \boldsymbol{x}_1(k) + \boldsymbol{B}_{dg} \boldsymbol{v}_c(k) + \boldsymbol{D}_{dg}(k) \boldsymbol{e}(k)\ . \tag{17}$$

Let us define the error state variable $\boldsymbol{E}(k)$ as

$$\boldsymbol{E}(k) = \boldsymbol{x}_1^*(k) - \boldsymbol{x}_1(k) \tag{18}$$

where $\boldsymbol{x}_1^*(k)$ is the reference grid-side current vector. To eliminate the steady-state error, an integral sliding surface function $\boldsymbol{S}(t)$ is selected as

$$\boldsymbol{S}(t) = \boldsymbol{E}(t) + \frac{k_I}{s} \boldsymbol{E}(t) \tag{19}$$

where k_I is the integral gain. This integral sliding surface can be discretized by using the relation as

$$s = \frac{2(1 - z^{-1})}{T_s(1 + z^{-1})}\ . \tag{20}$$

Then, the integral sliding surface function can be expressed in the discrete-time domain as follows:

$$\boldsymbol{S}(k+1) = \boldsymbol{E}(k+1) - \boldsymbol{E}(k) + \frac{k_I T_s}{2} \boldsymbol{E}(k+1) + \frac{k_I T_s}{2} \boldsymbol{E}(k) + \boldsymbol{S}(k)\ . \tag{21}$$

In general, the SMC suffers from the chattering phenomenon that causes current harmonics, increases power losses, and also produces severe electromagnetic compatibility noise in inverter applications. In order to eliminate such a chattering problem, the study in [21] gave the complete definition and detailed physical explanation for the quasi-sliding mode, in which a reaching condition is expressed as follows:

$$\boldsymbol{S}(k+1) - \boldsymbol{S}(k) = qT_s \boldsymbol{S}(k) - \varepsilon T_s \operatorname{sgn}(\boldsymbol{S}(k)),\ q > 0,\ \varepsilon > 0\ . \tag{22}$$

The control input of the ISMC can be obtained as

$$\boldsymbol{u}^* = \boldsymbol{u}_{eq} + \boldsymbol{u}_L + \boldsymbol{u}_N \tag{23}$$

where $\boldsymbol{u}_{eq}$ is the equivalent control, $\boldsymbol{u}_L$ is the linear control, and $\boldsymbol{u}_N$ is the nonlinear switching control. From (15), (18), (21), and (22), these control inputs can be obtained as follows:

$$\boldsymbol{u}_{eq} = \boldsymbol{B}_{dg}^{-1} \left[\boldsymbol{x}_1^*(k) - \boldsymbol{A}_{dg} \boldsymbol{x}_1(k) - \boldsymbol{D}_{dg} \boldsymbol{e}(k) + \frac{-2 + k_I T_s}{2 + k_I T_s} \boldsymbol{E}(k) \right] \tag{24}$$

$$\boldsymbol{u}_L = \boldsymbol{B}_{dg}^{-1}\left[\frac{2}{2+k_I T_s} qT_s \boldsymbol{S}(k)\right] \tag{25}$$

$$\boldsymbol{u}_N = \boldsymbol{B}_{dg}^{-1}\left[\frac{2}{2+k_I T_s} \varepsilon T_s \,\mathrm{sgn}(\boldsymbol{S}(k))\right]. \tag{26}$$

The proposed scheme also employs the resonant controllers of grid-side current for harmonic compensation. The resonant controllers are implemented in the SRF to take advantage of the simultaneous compensation for both the negative and positive sequence harmonics by one resonant term. Thus, the harmonically distorted grid at the 5th, 7th, 11th and 13th can be suppressed by compensating the harmonic components at 6th and 12th in the SRF. The transfer function of resonant controller is expressed as

$$R_{I2}(s) = \sum_{h=6,12} K_h \frac{s}{s^2 + (h\omega)^2} \tag{27}$$

where h denotes the harmonic order and K_h is the resonant gain. The transfer function of the resonant controller in (27) is implemented in the discrete-time domain by using the impulse invariant method. As shown in Figure 3, the grid-side current control loop generates the filter capacitor reference voltages $\boldsymbol{v}_c^*$ for the q- and d- axes. For the inner-loop capacitor voltage control and inverter-side current control, the PI controllers are employed with the estimated states.

4. SIMULATION AND EXPERIMENTAL RESULTS

In order to verify the feasibility and validity of the proposed current control scheme, the simulations have been carried out for an LCL-filtered three-phase grid-connected inverter based on the PSIM software. The system configuration and the proposed control scheme are depicted in Figure 2 and Figure 3. The system parameters are listed in Table 1.

Table 1. System parameters of a grid-connected inverter

Parameter	Value
DC link voltage	420 V
Grid voltage	220 V
Inverter-side filter inductance	1.7 mH
Grid-side filter inductance	0.9 mH
Filter capacitance	4.5 μF
Filter resistance	0.5 Ω
Load bank	24 Ω
Grid frequency	60 Hz
Switching frequency	10 kHz

Figure 4 shows the simulation results of the proposed current control scheme at steady-state under distorted grid condition. Figure 4(a) represents three-phase distorted grid voltages used for the simulations. The abnormal grid voltages contain the 5th, 7th, 11th, and 13th harmonic orders with the magnitude of 5% of the fundamental component. Figure 4(b) through Figure 4(d) shows the simulation results of using the proposed current control under the distorted grid voltages as in Figure 4(a). The reference value of the grid-side current is set to 7 A. Even though the grid voltages are severely distorted, the proposed control scheme provides a good harmonic compensation capability as can be observed from Figure 4(b), giving quite sinusoidal phase currents without noticeable distortion. Figure 4(c) shows the steady-state responses of the q-axis and d-axis grid-side currents at the SRF. As is shown, the grid-side currents track the reference values well, which indicates a good reference tracking performance of the proposed scheme. To verify the quality of injected grid currents, Figure 4(d) shows the Fast Fourier Transform (FFT) result for grid-side a-phase current. This figure also includes the harmonic limits specified by the grid interconnection regulation IEEE Std. 1547 [22]. As can be seen clearly, the harmonic components in the 5th, 7th, 11th, and 13th orders of the injected grid currents can be effectively damped by the proposed control scheme. The THD value of current is only 3.36%, which meets the quality criteria.

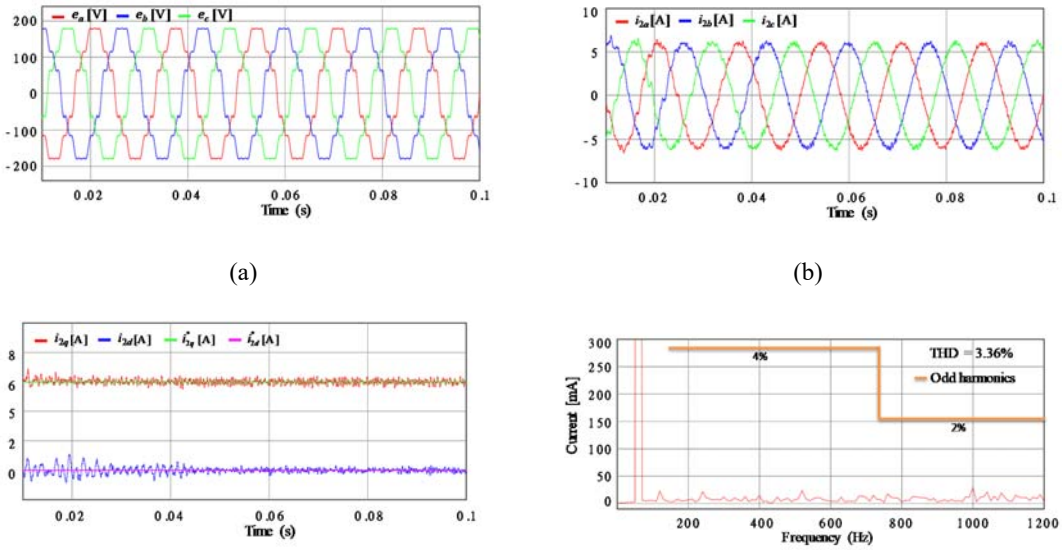

(a) (b)

(c) (d)

Figure 4. Simulation results for steady-state responses under distorted grid voltages with the proposed current control scheme (a) three-phase distorted grid voltages, (b) three-phase grid-side current responses, (c) grid-side current responses at the SRF, (d) FFT result for grid-side *a*-phase current

To demonstrate the transient performance of the proposed current control scheme, Figure 5 shows the simulation results under the same distorted grid condition as in Figure 4(a) when the *q*-axis grid-side current reference has a step change from 6 A to 10 A at 0.04 s, and again, from 10 A to 6 A at 0.07 s. Figure 5(a) and Figure 5(b) represent the transient responses of the grid-side currents at the natural reference frame and SRF, respectively. It can be clearly observed from these figures, except for small current oscillations during transient periods, the actual currents track the references rapidly and immediately reach new steady-state values. This indicates a good and fast transient response of the proposed control scheme.

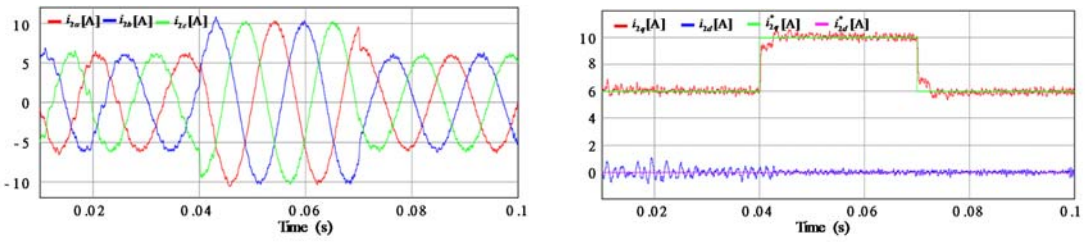

(a) (b)

Figure 5. Simulation results for transient responses under distorted grid voltages with the proposed current control scheme, (a) three-phase grid-side current responses, (b) grid-side current responses at the SRF

Figure 6 shows the simulation results for the inverter states and estimated states by using the discrete-time reduced-order state observer at the SRF. Obviously, the estimated states can follow the actual ones even under harmonic injection condition, which confirms a stable operation of the observer.

Figure 7 shows the simulation results for the estimated three-phase inverter-side currents and capacitor voltages at the natural reference frame. These estimation results clearly demonstrate a good estimating performance of the observer.

To verify the effectiveness of the proposed control scheme in practice, the experiments have been carried out. Figure 8 shows the configuration of the experimental system based on DSP TMS320F28335.

Figure 9 shows three-phase distorted grid voltages used for experimental evaluations. These grid voltages contain the 5th, 7th, 11th, and 13th harmonic orders with the magnitude of 5% of the fundamental component as the simulation in Figure 4(a).

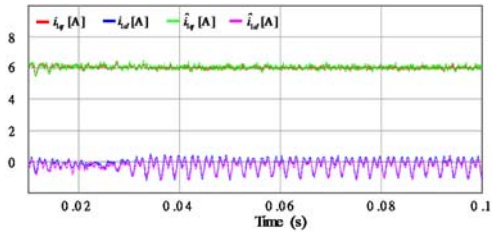

(a) Inverter-side currents and estimated states at the SRF

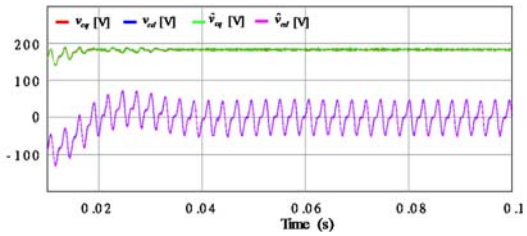

(b) Capacitor voltages and estimated states at the SRF

Figure 6. Simulation results for the estimating performance of the discrete-time reduced-order state observer, (a) Inverter-side currents and estimated states at the SRF, (b) Capacitor voltages and estimated states at the SRF

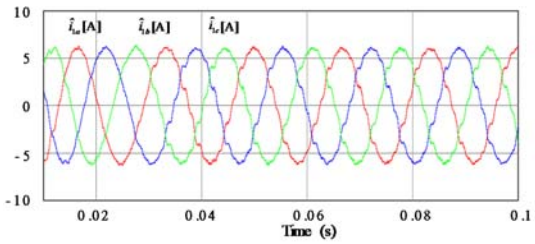

(a)

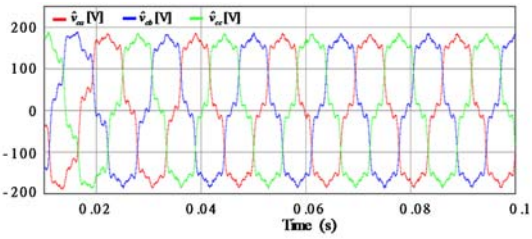

(b)

Figure 7. Simulation results for estimated three-phase states, (a) estimated three-phase inverter-side currents, (b) estimated three-phase capacitor voltages

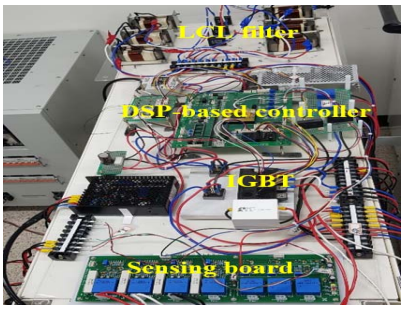

Figure 8. Configuration of the experimental system

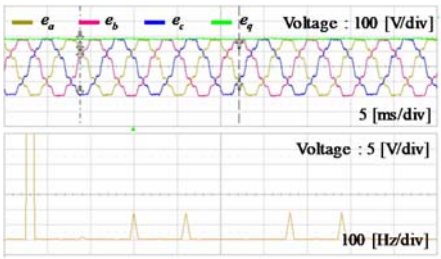

Figure 9. Three-phase distorted grid voltages used in experiments

Figure 10 shows the experimental results of the proposed current control scheme in terms of steady-state and transient responses under the distorted grid condition. It can be seen from Figure 10(a), the proposed control scheme provides considerably sinusoidal three-phase current waveforms at steady-state, which is consistent well with the simulation result in Figure 4(b). To evaluate the transient performance of the proposed control scheme, a step change in grid-side current reference from 4 A to 6 A is introduced. It can be observed from Figure 10(b) that the grid-side currents can track new references rapidly, which is also

matched with the behavior as shown in Figure 5(a). This confirms a good dynamic and steady-state performance of the proposed current control scheme in the presence of severely distorted condition of grid voltages.

Figure 11 shows the experimental results for the estimating performance of the discrete-time reduced-order state observe. In these figures, the estimated three-phase inverter-side currents and capacitor voltages are calculated in a DSP by using the estimated states at the SRF. Clearly, the experimental results are compatible with the simulation results in Figure 7, showing a good estimating performance.

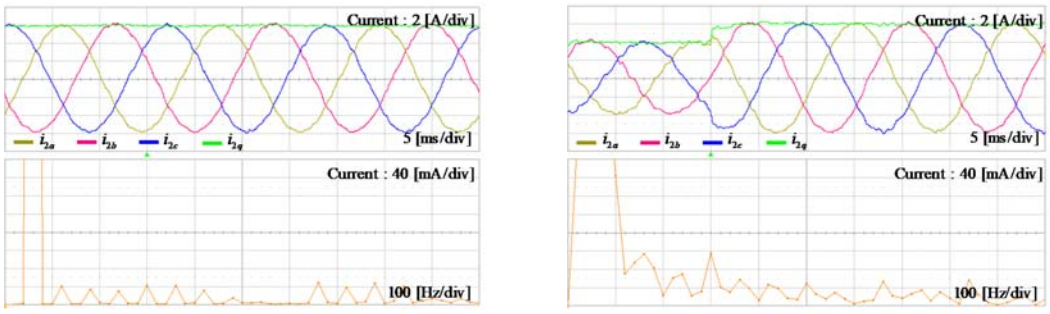

(a) (b)

Figure 10. Experimental results for the proposed current control scheme under distorted grid voltages, (a) steady-state response, (b) transient response

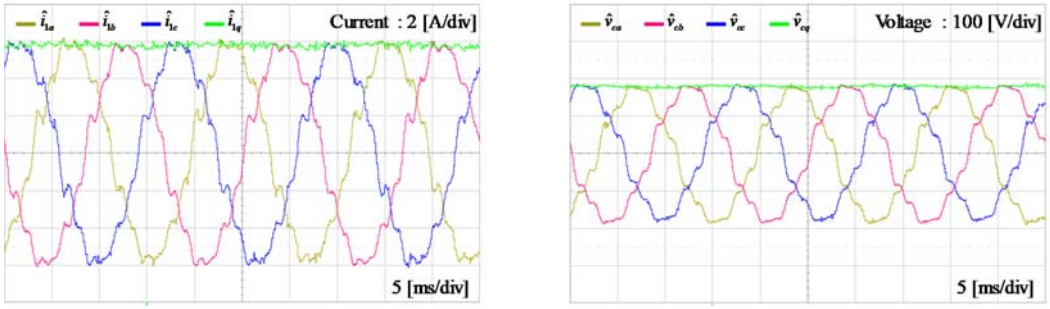

(a) (b)

Figure 11. Experimental results for the estimating performance of discrete-time reduced-order state observer, (a) Estimated three-phase inverter-side currents, (b) Estimated three-phase capacitor voltages

5. CONCLUSIONS

This paper has presented a multiloop indirect current control scheme for a three-phase LCL-filtered grid-connected inverter based on a discrete ISMC scheme and a resonant compensation. The proposed scheme is constructed by three cascaded control loops consisting of a grid-side current control, a capacitor voltage control, and an inverter-side current control. In general, to implement the multiloop current control scheme, many sensing devices should be required, which increases the cost and complexity of system. To overcome this limitation, a discrete-time reduced-order state observer is used to estimate both the inverter-side currents and capacitor voltages by using only the measured grid-side currents and grid voltages. This practically reduces the cost and complexity of an LCL-filtered grid-connected inverter system. For the purpose of suppressing the resonance behavior due to LCL filter, an active damping has been realized by means of the inverter-side current feedback loop. This approach is more feasible in comparison with the filter capacitor current feedback since the inverter-side current can be easily estimated by state observer. By integrating the capacitor voltage control loop into the control structure, the seamless transfer between the grid-connected mode and islanded mode is effectively achieved. To retain a high tracking performance and

robustness of the ISMC as well as an excellent harmonic compensation capability of the RC at the same time, these two control methods are combined in the proposed current control scheme. As a result, fast dynamic response, zero steady-state error, and robustness against the system uncertainties can be ensured by the proposed control. To verify the usefulness of the proposed control, a 2 kW prototype grid-connected inverter has been constructed and the whole control algorithm has been implemented on 32-bit floating-point DSP TMS320F28335. Comprehensive simulation and experimental results have been presented under distorted grid environment to demonstrate the usefulness of the proposed current control scheme.

ACKNOWLEDGEMENTS

This study was supported by the Research Program funded by the SeoulTech (Seoul National University of Science and Technology).

REFERENCES

[1] R. Chedid and S. Rahman, "Unit Sizing and Control of Hybrid Wind-Solar Power Systems," *IEEE Transactions on Energy Conversion*, vol. 12, pp. 79-85, 1997.
[2] R. Aboelsaud, A. Ibrahim, and A.G. Garganeev, "Review of Three-Phase Inverters Control for Unbalanced Load Compensation," *International Journal of Power Electronics and Drive Systems (IJPEDS)*, vol. 10, pp. 242-255, 2019.
[3] M. Pushpavalli and N. M Jothi Swaroopan, "Performance Analysis of Hybrid Photovoltaic/Wind Energy System Using KY Boost Converter," *International Journal of Power Electronics and Drive Systems (IJPEDS)*, vol. 10, pp. 433-443, 2019.
[4] J. G. de Matos, F. S. F. e Silva, and L. A. d. S. Ribeiro, "Power Control in AC Isolated Microgrids with Renewable Energy Sources and Energy Storage Systems," *IEEE Transactions on Industrial Electronics*, vol. 62, pp. 3490-3498, 2015.
[5] A. Molderink, V. Bakker, M. G. C. Bosman, J. L. Hurink, and G. J. M. Smit, "Management and Control of Domestic Smart Grid Technology," *IEEE Transactions on Smart Grid*, vol. 1, pp. 109-119, 2010.
[6] S. J. Yoon, N. B. Lai, and K. H. Kim, "A Systematic Controller Design for a Grid-Connected Inverter with LCL Filter Using a Discrete-Time Integral State Feedback Control and State Observer," *MDPI Energies*, vol. 11, pp. 1-20, 2018.
[7] F. Liu, X. Zha, Y. Zhou, and S. Duan, "Design and Research on Parameter of LCL Filter in Three-Phase Grid-Connected Inverter," *Proceedings of the 2009 IEEE 6th International Power Electronics and Motion Control Conference*, pp. 2174-2177, 2009.
[8] R. Peña-Alzola, M. Liserre, F. Blaabjerg, R. Sebastián, J. Dannehl, and F. W. Fuchs, "Analysis of the Passive Damping Losses in LCL-filter-based Grid Converters," *IEEE Transactions on Power Electronics*, vol. 28, pp. 2642-2646, 2013.
[9] Y. Jia, J. Zhao, and X. Fu, "Direct Grid Current Control of LCL-Filtered Grid-Connected Inverter Mitigating Grid Voltage Disturbance," *IEEE Transactions on Power Electronics*, vol. 29, pp. 1532-1541, 2014.
[10] R. Tirumala, N. Mohan, and C. Henze, "Seamless Transfer of Grid-Connected PWM Inverters between Utility-Interactive and Stand-Alone Modes," *Proceedings of the APEC. Seventeenth Annual IEEE Applied Power Electronics Conference and Exposition*, pp. 1081-1086, 2002.
[11] J. Kwon, S. Yoon, and S. Choi, "Indirect Current Control for Seamless Transfer of Three-Phase Utility Interactive Inverters," *IEEE Transactions on Power Electronics*, vol. 27, pp. 773-781, 2012.
[12] G. Shen, X. Zhu, J. Zhang, and D. Xu, "A New Feedback Method for PR Current Control of LCL-filter-based Grid-tied Inverter," *IEEE Transactions on Industrial Electronics*, vol. 57, pp. 2033-2041, 2010.
[13] H. S. Heo, G. H. Choe, and H. S. Mok, "Robust Predictive Current Control of a Grid Connected Inverter with Harmonics Compensation," *Twenty-Eighth Annual IEEE Applied Power Electronics Conference and Exposition (APEC)*, pp. 2212-2217, 2013.
[14] M. A. Abusara, M. Jamil, and S. M. Sharkh, "Repetitive Current Control of an Interleaved Grid-Tied Inverter," *2012 3rd IEEE International Symposium on Power Electronics for Distributed Generation Systems (PEDG)*, pp. 558-563, 2012.
[15] T. L. Tai and J. S. Chen, "UPS Inverter Design Using Discrete-Time Sliding-Mode Control Scheme," *IEEE Transactions on Industrial Electronics*, vol. 49, pp. 67-75, 2002.
[16] X. Hao, X. Yang, T. Liu, L. Huang, and W. Chen, "A Sliding-Mode Controller with Multiresonant Sliding Surface for Single-Phase Grid-Connected VSI with an LCL Filter," *IEEE Transactions on Power Electronics*, vol. 28, pp. 2259-2268, 2013.
[17] A. Chalanga, S. Kamal, and B. Bandyopadhyay, "A New Algorithm for Continuous Sliding Mode Control with Implementation to Industrial Emulator Setup," *IEEE/ASME Transactions on Mechatronics*, vol. 20, pp. 2194-2204, 2015.
[18] S. L. Jung and Y. Y. Tzou, "Discrete Sliding-Mode Control of a PWM Inverter for Sinusoidal Output Waveform Synthesis with Optimal Sliding Curve," *IEEE Transactions on Power Electronics*, vol. 11, pp. 567-577. 1996.
[19] S. W. Kang and K. H. Kim, "Sliding Mode Harmonic Compensation Strategy for Power Quality Improvement of a Grid-Connected Inverter under Distorted Grid Condition," *IET Power Electronics*, vol. 8, pp. 1461-1472, 2015.

[20] C. L. Phillips and H. T. Nagle, "Digital Control System Analysis and Design," Prentice Hall: Englewood Cliffs, NJ, 1995.
[21] W. Gao, Y. Wang, and A. Homaifa, "Discrete-time Variable Structure Control Systems", *IEEE Transactions on Industrial Electronics*, vol. 42, pp. 117-122, 1995.
[22] IEEE. IEEE Standard for Interconnecting Distributed Resources with Electric Power Systems; IEEE Std.1547; IEEE: New York, NY, USA, 2003.

BIOGRAPHIES OF AUTHORS

Seung-Jin Yoon was born in Seoul, Korea, in 1989. He received the M.S. degree in Electrical and Information Engineering from Seoul National University of Science and Technology, Seoul, Korea, in 2018. Currently he is working toward the Ph.D. degree in the Department of Electrical and Information Engineering at Seoul National University of Science and Technology. His research interests include renewable energy and power electronics.

Thanh Van Nguyen was born in Hai Duong, Vietnam, in 1994. He received the B. Eng. degree in Control and Automation Engineering from Hanoi University of Science and Technology, Hanoi, Vietnam, in 2017. Currently he is working toward the M.S. degree in the Department of Electrical and Information Engineering at Seoul National University of Science and Technology. His research interests include renewable energy and power electronics.

Kyeong-Hwa Kim was born in Seoul, Korea, in 1969. He received his B.S. degree from Hanyang University, Seoul, Korea, in 1991; and his M.S. and Ph.D. degrees from the Korea Advanced Institute of Science and Technology (KAIST), Daejeon, Korea, in 1993 and 1998, respectively, all in Electrical Engineering. From 1998 to 2000, he was a Research Engineer with Samsung Electronics Company, Korea, where he was engaged in the research and development of AC machine drive systems. From 2000 to 2002, he was a Research Professor with KAIST. From August 2010 to August 2011, he was a Visiting Scholar with the Virginia Polytechnic Institute and State University (Virginia Tech), Blacksburg, VA, USA. Since August 2002, he has been with the Seoul National University of Science and Technology, Seoul, Korea, where he is presently working as a Professor. His current research interests include AC machine drives, the control and diagnosis of power systems, power electronics, renewable energy, and DSP-based control applications. Professor Kim is a Member of the Korean Institute of Power Electronics (KIPE) and IEEE.